

Chirped pulse reflectivity and frequency domain interferometry in laser driven shock experiments

A. Benazzi-Mounaix,* M. Koenig, and J. M. Boudenne

*Laboratoire pour l'Utilisation des Lasers Intenses (LULI), Unité Mixte No. 7605, CNRS, CEA-Ecole Polytechnique,
Université Pierre et Marie Curie, 91128 Palaiseau, France*

T. A. Hall

Department of Physics, University of Essex, Colchester CO4 3SQ, United Kingdom

D. Batani, F. Scianitti, A. Masini, and D. Di Santo

Dipartimento di Fisica "G. Occhialini," Università degli Studi di Milano, Bicocca and INFM, Via Emanuele 15, 20126 Milano, Italy
(Received 2 April 1999)

We show the simultaneous applicability of the frequency domain interferometry and the chirped pulse reflectometry techniques to measure shock parameters. The experiment has been realized with the laser at the Laboratoire pour l'Utilisation des Lasers Intenses (LULI) with a 550-ps pulse duration and an intensity on target $\sim 5 \times 10^{13} \text{ W/cm}^2$ to produce a shock in a layered aluminum-fused silica target. A second low energy, partially compressed chirped probe beam was used to irradiate the target rear side and the reflected light has been analyzed with a spectrometer, achieving a temporal resolution of the order of 1 ps.
[S1063-651X(99)50509-6]

PACS number(s): 52.50.Jm, 44.30.+v, 52.35.Tc

I. INTRODUCTION

Many recent experiments [1–5] have been devoted to the study of laser driven shock waves and their use in the equation of state (EOS) measurement of strongly compressed materials, a subject of current interest and of great importance both for inertial confinement fusion (ICF) and astrophysics [6]. For example, EOS models can affect the fuel compression estimated by simulations and produce different scenarios of stellar evolution or different description of planet interiors.

It is well known that absolute EOS measurements require the simultaneous measurement of two shock parameters. The shock velocity D can be easily measured with relatively a good precision [2,7]. The feasibility of the simultaneous measurement of D and the fluid velocity U has recently been demonstrated, provided that a very high power laser with a long pulse is available [3]. The first measurement of these two quantities has been performed in a transparent medium (liquid deuterium [6]), but up to now such type of measurement has not been performed in opaque media. A recent work by Evans *et al.* [8] showed the possibility of measuring the fluid velocity of shocked aluminum relaxing the constraint on laser power, by using the frequency domain interferometry (FDI) technique [9]. They also deduced the shock velocity by measuring the shock breakout time with targets of different thickness. In their case, the shock was highly nonstationary, being produced by a 120-fs laser pulse, and the two quantities were obtained from the analysis of different shots, by assuming that shot to shot energy fluctuations

were negligible. Moreover, the probe beam was also very short and consequently gave a 120-fs snapshot only of the shock breakout. Then in order to reconstruct the time evolution of the fluid velocity, many shots were necessary.

Other works on equation of state tried instead to measure the material temperature by using the space resolved optical pyrometry technique [10,11]. The problem, in this case, is that it requires additional modeling to interpret the experimental data.

Therefore, the development of new diagnostics is important not only to determine the second parameter but also to increase the accuracy in the measurements. Precision is indeed the crucial point in EOS measurements, discrimination between different theoretical models requiring shock velocity (and/or fluid velocity) data accurate to a few percent or less. In the past, when the matter could be compressed in the multimegabar range by nuclear explosions only, EOS measurements were not clean enough to achieve a good precision. The possibility to perform very high quality shocks with lasers [1,2], and to use them in EOS experiments with a few percent measurement error has been recently demonstrated [5,7,12]. However, constant efforts are currently devoted to improving their accuracy.

Recently the velocity interferometry (VISAR) technique, developed by Barker and Hollenbach [13] to measure the time history of the shock velocity, has been applied to determine the deuterium EOS [14]. Even if a high precision on the instantaneous value of velocity was obtained, their quite low temporal resolution (>75 ps) did not allow to observe several important phenomena such as the presence of pre-heating (or of any other shock precursors) and the nonequilibrium structure of the shock front, in particular the relaxation of ions and electrons. An alternative method was proposed, but not implemented, by Gold *et al.* [15] to obtain a good precision on the shock or fluid velocity and at the

*Present address: CEA/DSM/DAPNIA/ Service d'Astrophysique, Bat. 709, Center d'Etudes de Saclay, L'Orme des Merisiers F-91191, Gif-sur-Yvette Cedex, France.

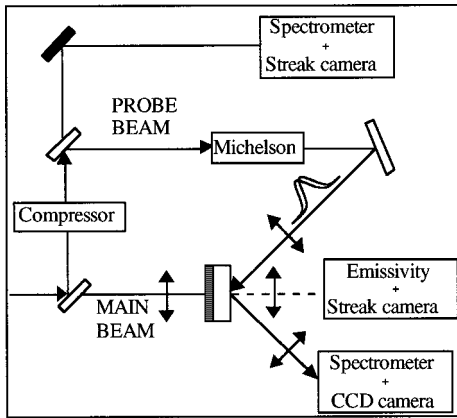


FIG. 1. Experimental setup.

same time to reach a very high temporal resolution. This is the chirped pulse reflectometry (CPR) technique in which the probe beam reflection from the target rear side is spatially and spectrally resolved. Such a method is based on using a chirped optical laser probe to determine the shock breakout time. Frequency chirp in the probe pulse gives a univocal relation between the instantaneous frequency and time. The time at which shock breakout takes place is hence characterized by a sharp drop in reflectivity at a given wavelength. Therefore the CPR technique is an alternative method to measure shock breakout time. With respect to the usual streak camera diagnostic whose typical resolution is about 10 ps, it also offers the possibility of higher temporal resolution, potentially <1 ps [15]. Temporal accuracy depends on the ratio of the spectral bandwidth and the pulselength of the beam (i.e., $\Delta\lambda/\Delta\tau$).

In this Rapid Communication we present the feasibility of a method based on the simultaneous use of the FDI and the CPR techniques. This method allows, *on the same laser shot*:

- (i) The very precise determination of the shock breakout time thanks to the high temporal (and spatial) resolution typical of the CPR technique.
- (ii) The precise measurement of the fluid velocity U and/or the shock velocity D (depending on the experimental conditions) as a function of time with a laser of relatively "small" dimensions ($E_{2\omega} \approx 30$ J in 550 ps).
- (iii) To check the quality of the shock front and to observe microstructures not observable with the usual streak camera time resolution.

II. EXPERIMENTAL TECHNIQUE AND SETUP

In this experiment (see Fig. 1), we used two beams both obtained from the 100 TW LULI laser. The first one, at high energy, was an uncompressed (FWHM ≈ 550 ps) chirped pulse doubled in frequency (central wavelength $\lambda_{2\omega} = 0.5285$ μm) which generated the shock wave in the target. The target was made of a 4 μm layer of CH (laser side), and 10 μm of Al coated on 2 mm of fused silica (rear side of the target). The plastic layer was used to minimize preheating effects. The laser pulse was focused by a $f=250$ mm lens onto the target and optically smoothed with RPP. The characteristics of our optical system (RPP+focusing lens) were such that a focal spot was 200 $\mu\text{m} \times 400$ μm (FWHM). This

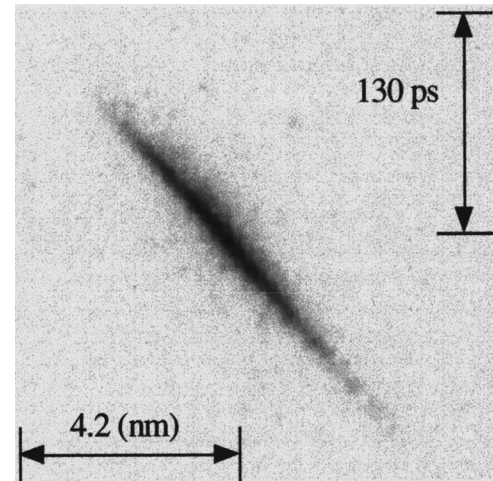


FIG. 2. Typical image obtained with a spectrometer coupled with a streak camera. This diagnostic allows one to check the time dependence of the chirped, partially compressed, probe pulse.

allowed a large dimension of the shocked region to be obtained while maintaining a high intensity ($\sim 5 \times 10^{13}$ W/cm 2). The second beam, at low energy, was a partially compressed chirped probe beam which irradiated the target rear side.

First, a diagnostic based on a visible spectrograph coupled with a streak camera allowed us on each shot to check the chirp of the beam, namely, the frequency or wavelength dependence on time. In our case we verified that $\Delta\lambda \ll \lambda_0$, where $\Delta\lambda$ is the spectral width and λ_0 the wavelength of the probe, and that the chirp was linear to a good approximation (see Fig. 2). From the measurement of $\Delta\lambda$ and the pulse duration $\Delta\tau$ (FWHM ~ 75 ps) we obtained the relation $\lambda(\tau) = \lambda_0 + \alpha t$, where $\alpha = \Delta\lambda/\Delta\tau$. The probe beam, before irradiating the target at 45°, was passing through a Michelson interferometer (as shown in Fig. 1) to produce a pair of collinear probe pulses separated by $\Delta t = 10$ ps. To improve the spatial quality of the probe beam, a system of two slits (image relayed) was used before focusing it on the target with a f/4 lens. This is equivalent to a spatial filter but guarantees a higher level of luminosity.

The main diagnostic was based on imaging the probe light reflected from the interface aluminum-quartz interface onto the entrance slit of a high resolution visible spectrograph by using a f/4 objective. A 12 bit charge-coupled device (CCD) was placed on the output plane of the spectrometer as a detector. The magnification of the imaging system was 10, resulting in a spatial resolution of ≈ 4 μm in the target plane. Before the shock breakout the two probe beams are reflected on the unperturbed Al-SiO₂ interface. In this case the spectrograph gives the fringe pattern caused by the interference in the frequency domain of the two temporally separated beams. After the shock breakout, the fringe pattern moves because of the phase shift between the two probe beams. Therefore, this diagnostic allowed us to measure both the amplitude variations and the phase shift of the reflected light induced by the modification of the optical properties of the perturbed material and by the motion of the reflecting surface. Moreover, the chirp of the two beams makes it possible to use the spectral axis of the spectrograph as a time scale and hence get the phase shift as function of time. A comple-

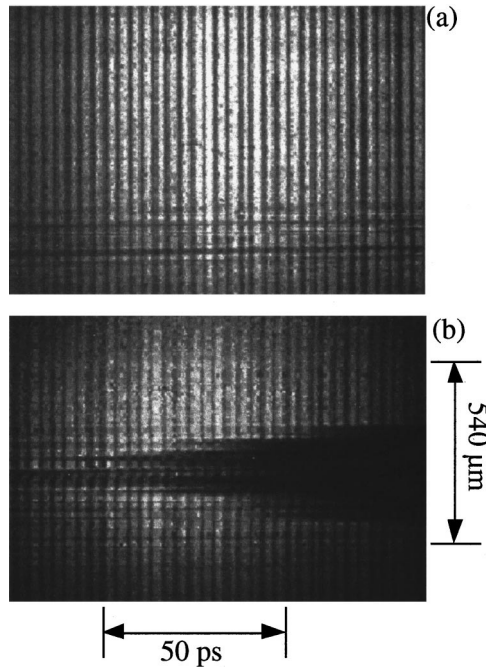


FIG. 3. Experimental images obtained with the spectrograph, representing the interference pattern of the two probe chirped pulses. The horizontal axis represents both the wavelength and the time scale. (a) Image of reference, with only the probe beam. (b) Image with the probe and the main beam generating the shock in the aluminum.

mentary diagnostic (see Fig. 1), based on a visible streak camera, recorded the target rear side emissivity. It was used to check the shock quality and the breakout time with respect to a time fiducial beam. An optical system made of an objective and two lenses imaged the target rear face onto the slit of the streak camera with a magnification $M = 12$, resulting in a spatial resolution of $8 \mu\text{m}$ at the target plane. The streak camera temporal resolution was of $\approx 20 \text{ ps}$.

The synchronization of the probe beams with the shock arrival time at the target rear side, was performed in two steps. First, we synchronized the probe and the main beam by using a streak visible camera (see Fig. 1). Second, we measured the time delay between the main beam and the shock arrival time using the rear side emissivity diagnostic. Therefore, we were able to have an absolute synchronization on one shot. The purpose was to have the shock breakout time near the center of the probe pulse (75 ps duration), so to be able to measure the reflectivity before, as well as after, the shock breakout. A delay line was used to adjust the probe beam timing, according to the thickness of the target and to the laser energy.

III. RESULT ANALYSIS

Before each shot, a reference shot was performed by using only the probe beam. A typical image obtained with the spectrograph is shown in Fig. 3(a). The horizontal cut represents the Fourier transform in the frequency domain of the sum of two chirped pulses (more precisely the squared modulus of the Fourier transform). It is important to notice that we are in the limit $\Delta\omega\Delta\tau\gg 1$ since the relation between $\Delta\omega$ and $\Delta\tau$ is given by $\Delta\omega=\beta\Delta\tau$, where β is related to the

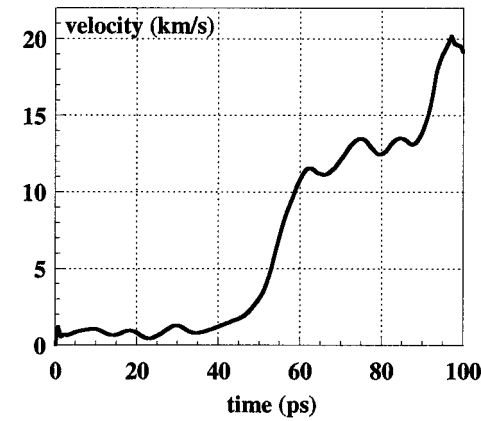


FIG. 4. Deduced velocity as a function of time.

chirp coefficient α by $\beta=\alpha\omega_0^2/(2\pi c)$ (we recall that for Fourier transform limited laser pulses we have instead $\Delta\omega\Delta\tau\approx 1$). The total spectral width is consistent with the one measured with the streak camera (Fig. 2). The interfringe distance depends on the pulse separation (i.e., $\Delta\tau$), and is well reproduced by an analytical calculation. With our chirp (i.e., α) and pulse separation, we reached a temporal resolution much better than 3 ps, corresponding to the fringe width.

We show an image with a shock breakout obtained with the spectrograph in Fig. 3(b). The results emphasize some nonuniformities in the front shock on very small scales, connected to the small size speckles produced by the RPP. This is possible thanks to the very high temporal achieved with the CPR technique, while the corresponding streak image shows a quite uniform shock breakout, due to much lower time resolution. From the image of Fig. 3(b), one can measure the phase shift associated with the motion of the reflecting surface as function of time and deduce its velocity. If we consider the interface moving with a velocity U , the Doppler phase shift is $d\Phi/dt=4\pi Un\cos\theta/\lambda_0$ where n is the refractive index of the quartz and θ is the probe beam incident angle. In order to determine the phase shift, we used an automatic procedure developed by Geindre [16], which considers an arbitrary zero phase point given by the reference image [Fig. 3(a)], and at each following time gives the total phase.

Figure 4 shows the time behavior of the deduced velocity. When the shock arrives at the interface, a shock with approximately the same velocity is transmitted into the quartz (the impedance of the Al and the quartz is approximately the same).

In Fig. 4, we can distinguish three different phases:

(1) For $t < 50 \text{ ps}$ the probe beam is reflected on the unperturbed aluminum-quartz interface. The observed noise on the velocity corresponds to one pixel on the CCD camera.

(2) For $50 \text{ ps} < t < 80 \text{ ps}$ we found $U \approx 12.5 \text{ km/s}$. This corresponds to the interface velocity between aluminum and quartz and due to the continuity of the Rankine-Hugoniot relations, to fluid velocity in both materials. Therefore, according to SESAME tables [17], the shock pressure in aluminum is $P \approx 7 \text{ Mbar}$ as expected with our laser intensity. Here, the quartz is partially transparent and the probe beam is reflected at the interface, after going through the compressed quartz. The variation of the refraction index of compressed

silica [18,19] should be, in principle, considered in deducing the above fluid velocity. However, in our case very small thickness of the shocked silica (lower than one laser wavelength) allows us to neglect this effect [8]. We finally considered the phase shift, due to the reflection at the aluminum surface under shock conditions.

(3) About 35 ps after the shock breakout, a higher velocity is observed. We think that this corresponds now to the reflection from the shock front in fused silica. We measured $D \approx 19$ km/s, which is consistent with the fluid velocity $U \approx 12.5$ km/s obtained. Such velocity is not observed in the first phase because the thickness of the compressed silica increases with time as $(D-U)t$ and its absorption grows exponentially with such thickness, thereby quickly screening the Al/SiO₂ interface. At the same time, there is an augmentation of the electronic conduction, confirmed by an increase of the measured reflectivity. The strong shock compression induces either a plasma phase or metal transition.

The relative error on the determination of such velocities is equal to $\Delta\Phi/\Phi$, where $\Delta\Phi$ is ± 0.17 rad, and Φ is the total phase change. Hence, in principle, errors as small as $\pm 0.3\%$ can be obtained.

IV. CONCLUSIONS

In conclusion, we have shown the applicability of the simultaneous use of the FDI and the CPR techniques to measure shock parameters. A high temporal resolution of the order of 1 ps has been achieved. If step targets are used, this method could be applied to measure the shock breakout time (and then the shock velocity), with a temporal precision much better than with a streak camera. Also fluid velocity can be simultaneously measured provided the back transparent layer does not metalize. Another important advantage of this technique is that it allows one to evidence the presence of hot spots in the laser beam and their effects on the local shock breakout and preheating.

ACKNOWLEDGMENTS

This work was supported by the EU TMR program under Contract No. ERBFMGE-CT95-0044. We would like to thank J. P. Geindre and J. C. Gauthier for fruitful discussions on this work.

[1] Th. Löwer *et al.*, Phys. Rev. Lett. **72**, 3186 (1994).
 [2] M. Koenig *et al.*, Phys. Rev. E **50**, R3314 (1994); D. Batani *et al.*, Laser Part. Beams **14**, 211 (1995).
 [3] L. Da Silva *et al.*, Phys. Rev. Lett. **78**, 483 (1997).
 [4] R. Cauble *et al.*, Phys. Plasmas **4**, 1857 (1997).
 [5] A. Benuzzi *et al.*, Phys. Rev. E **54**, 2162 (1996).
 [6] G. Collins *et al.*, Science **281**, 1178 (1998).
 [7] M. Koenig *et al.*, Phys. Rev. Lett. **74**, 2260 (1995).
 [8] A. M. Evans *et al.*, Phys. Rev. Lett. **77**, 3359 (1996).
 [9] J. P. Geindre *et al.*, Opt. Lett. **19**, 1997 (1994).
 [10] L. Da Silva, A. Ng, and D. Parfeniu, J. Appl. Phys. **58**, 3634 (1985).
 [11] T. Hall *et al.*, Phys. Rev. E **55**, R6356 (1997); S. Bossi *et al.*, Laser Part. Beams **15**, 485 (1997).
 [12] M. Koenig *et al.*, Appl. Phys. Lett. **72**, 1033 (1998).
 [13] L. M. Barker and R. E. Hollenbach, J. Appl. Phys. **43**, 4669 (1972).
 [14] P. M. Celliers, G. W. Collins, L. B. D. Silva, D. M. Gold, and R. Cauble, Appl. Phys. Lett. **73**, 1320 (1998).
 [15] D. M. Gold, A. Sullivan, R. Shepard, J. Dunn, and R. Stewart (private communication).
 [16] J. P. Geindre (private communication).
 [17] SESAME: The LANL Equation of State database, Los Alamos National Laboratory Report No. LA-UR-92-3407, 1992.
 [18] R. E. Setchell, J. Appl. Phys. **50**, 8186 (1979).
 [19] B. Marler *et al.*, Phys. Chem. Miner. **16**, 286 (1988).